An axial molecular-beam diode laser spectrometer

Hans D. Osthoff and Wolfgang Jäger[a)]
Department of Chemistry, University of Alberta, Edmonton, Alberta T6G 2G2, Canada

Johnathon Walls and William A. van Wijngaarden
Department of Physics and Astronomy, York University, Toronto, Ontario M3J 1P3, Canada

(Received 9 June 2003; accepted 20 October 2003)

A mid-infrared tunable diode laser molecular-beam spectrometer for the purpose of trace gas sensing and the study of van der Waals complexes is described. The spectrometer employs a Herriott multipass cell with up to 72 passes. The sample gas is injected parallel to the optical axis through a hole at the center of the far mirror. The molecular absorption is Doppler split, resulting from the laser beam propagating parallel and antiparallel to the molecular-beam expansion. The axial expansion leads to narrower line widths and increased sensitivity, compared to the traditional vertical injection method, as a result of selective sampling of the central part of the molecular expansion with reduced Doppler broadening and longer residence time of the molecular sample in the laser beam. The molecular expansion leads also to selective signal enhancement of low-J transitions, as demonstrated for the ν_3 antisymmetric stretch vibration of CO_2. A microwave horn antenna was implemented into the spectrometer to enable microwave–infrared double-resonance experiments. The spectrometer performance was evaluated by recording spectra of the CO_2–Ar, $(CO_2)_2$, CO_2–He, and CO_2–SO_2 van der Waals complexes near the $R(0)$ transition of the ν_3 band of CO_2 around 2349 cm^{-1}. The feasibility of using a pulsed molecular expansion for trace gas sensing is explored. [DOI: 10.1063/1.1634364]

I. INTRODUCTION

Mid-infrared tunable diode laser spectrometers are employed in a number of laboratories to measure high-resolution ro-vibrational spectra of weakly bound complexes for the study of weak intermolecular interactions.[1–4] Typically, lead salt diode lasers that operate continuously at cryogenic temperatures are the radiation source in these instruments, but quantum cascade lasers with higher operating temperatures show promise.[5] Multipass cells of Herriott,[6,7] White,[8] Perry,[9] or astigmatic[10] designs increase the absorption path length and lead to significant sensitivity enhancement. Various modulation schemes, including the fast scanning technique,[1] have been introduced to further increase the instrument sensitivity.

Weakly bound complexes, or van der Waals clusters, can be generated and stabilized in supersonic free jet expansions. Most common are pulsed molecular expansions with significantly less sample consumption than continuous beams. The pulsed sample introduction results in an additional on/off modulation that can be used for signal detection and background subtraction. The molecular beam is usually injected perpendicularly to the optical axis. If commercially available nozzles with circular orifice are used, significant Doppler broadening of the absorption lines occurs mainly because of the large spatial divergence of the expansion. The Doppler broadening can be reduced, and the absorption path length increased, if somewhat more complex slit nozzles are used.[4,11]

Mid-infrared tunable diode laser spectrometers are also used in atmospheric trace-gas-sensing applications.[12–17] In this case, the sample gas is often continuously pumped through a multipass cell under reduced pressure or, in the case of aircraft-mounted instruments, sampled *in situ* in the reduced pressure environment at high altitude. The lower pressure leads to narrower linewidths and less overlap with atmospheric water and CO_2 lines.

The current study was undertaken to explore the applicability of a molecular expansion in a mid-infrared diode laser spectrometer for atmospheric trace-gas sensing. For this purpose, we assembled a molecular-beam tunable diode laser absorption spectrometer. We employ a commercially available pinhole nozzle and use it in a configuration such that the optical axis of the Herriott multipass cell and the molecular expansion are parallel. Such a parallel arrangement is often used in microwave Fourier transform spectrometers,[18–20] and has recently also been applied in a millimeter-wave spectrometer.[21] The expectations from such a setup in a mid-infrared spectrometer are a gain in sensitivity and narrower linewidths. The increased sensitivity is anticipated to result from greater overlap of the expanding gas with the laser beam, and the reduced linewidth from selective sampling of the central part of the molecular expansion with a narrower velocity distribution.

In this article, the performance of the instrument is evaluated with the laser operated in fast scan mode,[1] and the suitability of the spectrometer as a tool to study weakly bound complexes in the mid-infrared is demonstrated. A microwave–infrared double-resonance (MW-IR DR) setup was implemented as a spectroscopic assignment tool. In addition, we propose the use of our molecular beam spectrom-

a)Electronic mail: wolfgang.jaeger@ualberta.ca

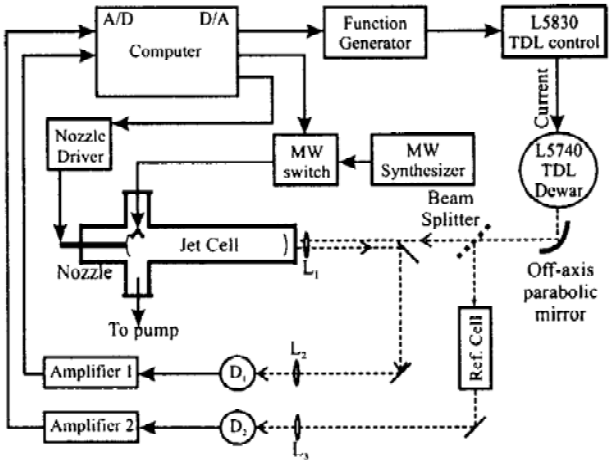

FIG. 1. Schematic diagram of the spectrometer layout.

eter as a way to enhance selectivity and sensitivity in trace-gas-sensing applications. For this purpose, a unique frequency modulation scheme was developed and evaluated. The redistribution of the energy level population into lower levels in the molecular beam is not only expected to remove most interference from atmospheric water and CO_2, but also to enhance sensitivity, especially for large system with many thermally accessible states.

II. EXPERIMENTAL PROCEDURE

A. Fast sweep method

1. Description of instrument

An earlier version of the instrument has been described elsewhere.[22] A schematic diagram of the instrumental configuration is shown in Fig. 1. A tunable lead salt semiconductor diode, capable of operating near 2349 cm^{-1} in single-mode over a range of several wave numbers (Laser Components F-2462-GMP), is housed in a liquid-nitrogen-cooled (LNC) dewar (Laser Photonics L5740). The laser temperature is controlled by a Laser Components L5830 control unit, which also acts as the current source. A Stanford Research Systems Function Generator (DS345) is used to generate the laser current modulation signal. The laser beam is focused by an off-axis parabolic mirror. For improved performance, the optical elements outside the vacuum system are kept under nitrogen to reduce atmospheric absorption. Part of the beam (~8%) is diverted by a pellicle beam splitter (Oriel Instruments 37400) and passed through a 10-cm-long reduced-pressure reference cell for frequency calibration. Alternatively, a 2.54-cm-long temperature-stabilized germanium tuning rate etalon (Laser Analytics L5940) can be employed. The calibration beam is focused with a 100 mm focal length CaF_2 lens (Janos Technologies A1404-110) onto a LNC InSb detector (Infrared Associates). The main beam (92%) is mildly focused using a 500 mm focal length CaF_2 lens (Janos Technologies, A1404-350) and enters, through a CaF_2 Brewster angle window, the vacuum chamber that houses the multipass sample cell. The multipass cell mirrors are 50.8-mm-diameter gold-coated mirrors with either 101.6 or 508.0 mm focal lengths (Edmund Industrial Optics K32-816 or K32-822). The spherical mirrors were kept at a distance of just below twice their common focal length, resulting in up to 72 passes of the laser beam, corresponding to a total absorption path length of up to 64 m. Optical fringing is greatly reduced in the multipass cell by following the recommendations of McManus *et al.*[23] The vacuum chamber is evacuated by a LNC diffusion pump (Edwards Diffstak® CR160-700) backed by a dual-stage backing pump (Edwards E2M18). The sample gas is injected into the sample cell using a pulsed nozzle (General Valve, Series 9) with an in-house-constructed aluminum nozzle head with spherical orifice (diameter 0.8 mm). The nozzle can be moved to a position perpendicular to the optical axis, but is commonly placed along the optical axis, with the nozzle head sitting in a 5 mm coupling hole in one of the mirrors. The nozzle is controlled by a custom-made pulsed nozzle driver (CPC Consulting, PND-2). The laser beam enters and exists the Herriott multipass cell through a coupling hole in the second mirror at slightly different angles. The existing beam is focused with a 75 mm focal length CaF_2 lens (Janos Technologies A1407-3081) onto an InSb detector (Electro-Optical Systems IS-010-LN4). Both main and reference signals are amplified using fast (dc to 250 kHz) amplifiers and a/d-converted and stored using a dual-channel, 12-bit, 50 MS/s PCI data acquisition board (Gage CompuScope 1250). Data acquisition and the operation of the spectrometer are controlled by a personal computer, using software written in Delphi 5 and control signals generated with an Iotech DaqBoard™ 2000 I/O card.

For MW-IR DR experiments, an *X*-band microwave horn antenna is mounted perpendicularly to the optical axis near the nozzle head. A Watkins–Johnson 1250 synthesizer is used as the microwave source. The microwave pump signal is on/off-modulated with a microwave $p-i-n$ diode switch (SMT SFS0518).

2. Operation

The lead salt diode laser is operated in rapid scanning mode in a similar fashion as described by De Piante *et al.*[1] The current applied to the diode laser and therefore the output frequency is modulated using the Stanford Research Systems function generator. Upon triggering, the function generator delivers a series of typically several hundred positive 1-ms-long linear voltage ramps, separated by short recovery periods. Typical scan rates are 850 $cm^{-1}\,s^{-1}$. During data acquisition and subsequent transfer from board to PC memory, the current modulation remains uninterrupted. This has the dual advantage of stabilizing the effect of ohmic heating on the laser diode and allowing the accumulation of several scans within a single gas pulse. It also improves the overall reproducibility of the frequency scan. The laser scan rate is limited by the onset of asymmetric peaks due to frequency limitations of the detection electronics (~250 kHz) and the detector rise time (~1 MHz). In a typical experiment, the full width at half-maximum (FWHM) of a line is scanned in about 4 μs.

After installation of a new diode, the laser current and temperature are adjusted to produce single-mode output of the diode, monitored using the etalon scan. Multimode lasing action is visible by a second set of fringes superimposed on

the main fringing pattern. Mode hops are usually harder to spot, but often cause an abrupt phase shift in the periodic etalon output. In general, single-mode lasing is more likely when the laser is operated near threshold conditions. Single-mode diode operation is advantageous because it eliminates the need for a monochromator, whose insertion would result in a significant reduction of effective laser power. Absolute frequencies are determined by comparing the spectrum of a reference gas at a few Torr pressure with a simulated spectrum based on the Hitran[24] database. This can be a tedious task, especially since the gaps between laser modes frequently exceed several wave numbers. Once the lasing behavior of the diode is characterized, its operation becomes relatively straightforward. The lasing characteristics of the diodes we tested did not change over the period of many months. One of our diodes in particular emits laser light in single mode (confirmed by a clean etalon fringing pattern) near the R(0) line of the ν_3 fundamental transition of carbon dioxide at 2349.917 cm^{-1}. We decided to work in this spectral region in all experiments described here.

In a typical experiment, data from the sample cell and from the reference cell are acquired at sampling rates of 25 MHz. A scan is stored in up to 38 000 data points per channel, corresponding to an average lifetime of the molecular expansion in He carrier gas of approximately 1.5 ms. The collected spectra are therefore also a record of the time evolution of the molecular expansion. The frequency sweep can be repeated several times during a single molecular pulse depending on the lifetime of the molecular beam. The end of the molecular expansion is signaled by the disappearance of characteristic Doppler doublets, a result of the coaxial expansion, and by the appearance of CO_2 monomer transitions. Since the pulse repetition rate is only 5–10 Hz, limited by the pumping speed of the diffusion pump, data processing can take place immediately between pulses.

A typical experiment begins with the simultaneous acquisition of two spectra, which are stored in separate acquisition channels. The background spectrum is taken without injection of a molecular pulse, that is, with the empty sample cell, and is used for background subtraction of the molecular spectrum. The reference spectrum is that of the CO_2 reference cell and is stored in the second channel of the data acquisition card. The pulse nozzle is then triggered after a 500 μs delay, and two new spectra, a molecular spectrum and a reference spectrum, are recorded. The earlier recorded background spectrum is subtracted immediately after acquisition of the molecular spectrum. The shift of the new reference spectrum of the CO_2 reference cell with respect to the original reference spectrum is determined and used in a software-locking scheme to offset any frequency drift. Subsequent scans of the reference spectrum are averaged with previous scans for improved performance. The entire data acquisition cycle is repeated until a satisfactory signal-to-noise ratio (SNR) is obtained.

For long-term data acquisition, gradual instrument drifts are known to become the limiting source of noise. In our instrument, a long-term frequency lock is maintained by shifting subsequent reference spectra relative to the initial reference spectrum before co-addition. The shift (that is, the number of data points s) is determined by an iterative algorithm designed to find a local minimum to the function

$$f(s,c)=\sum_{i=a}^{b}[x_n(i+s)-x_{\mathrm{ref}}(i)+c]^2, \tag{1}$$

with respect to both s and c. The term c corrects for a variable dc offset of the ac-coupled reference channel. The array of data points $x_n(i)$ contains the nth digitized reference spectrum, and the array $x_{\mathrm{ref}}(i)$ contains the reference spectrum.

For MW-IR-DR experiments, a molecular pulse is injected into the sample cell for both background and main scan. The microwave switch is closed for the acquisition of background spectra and opened for DR spectra. This type of on/off modulation results in spectra showing only DR effects.

3. Post-acquisition data processing

The SNR can be improved by post-data-acquisition digital filtering. Simple 25-point boxcar averaging was employed throughout. In addition, we explored several other digital filters, including modifications of the Wiener[25] and Kalman[26] algorithms. While the performance of the Kalman filter was on occasion impressive, we found that optimization of sample conditions, elimination of optical fringing and accumulation of more frequency scans were generally more effective in improving the SNR.

Absolute frequencies were determined from the simultaneously recorded CO_2 reference spectra. The parameters of Gaussian functions were fitted to individual lines with precisely known[24] center frequencies. A sixth- to eighth-order polynomial was then used to describe the tuning behavior of the laser diode, and a calibration curve relating absolute frequency and data points was constructed.

Transitions in the molecular beam were easily identified by the characteristic Doppler splitting. In order to determine the rest frequencies, a Gaussian expression was fitted to the observed Doppler pair. Line widths, amplitudes, Doppler splitting, and center frequencies were the fitting parameters. Lorentzian expressions were also used for data analysis, giving the same center frequencies and Doppler splittings as from the Gaussian expressions.

B. Single-frequency method

1. Description of instrument

For single-frequency monitoring, the instrument is only slightly changed from the version described in Sec. II A 1 by the implementation of different frequency-locking and modulation schemes. The output of the reference detector is demodulated with a lock-in amplifier (Ithaco Dynatrac 391A). The demodulated reference signal is then used in a feedback loop to stabilize the frequency of the laser diode. The main signal is demodulated with a Stanford Research Systems 830 phase-sensitive detector before it is processed in the data acquisition board.

2. Operation

For single-line monitoring, the laser diode needs to be locked to a low-J transition of the analyte gas. For this work,

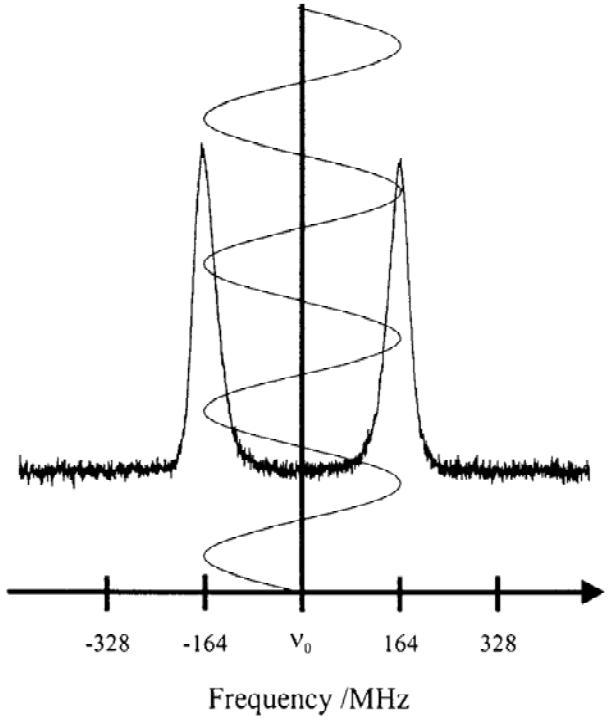

FIG. 2. The frequency modulation signal superimposed on the Doppler split R(0) transition of CO_2. The modulated signal is centered at the rest frequency ν_0 of the CO_2 transition and the modulation depth is set such that it reaches both Doppler components.

the diode was locked to the R(0) transition of CO_2 at 2349.917 cm^{-1}. A 51 kHz sinusoidal signal is used to modulate the output of the laser diode. The modulation depth is set such that it reaches both Doppler components of the monitored transition for a specific sample backing pressure and sample composition (Fig. 2). The absorption signal is thus observed at twice the input frequency. The lock-in amplifier is operated in 2 f-demodulation mode, using time constants of either 300 μs or 1 ms. In contrast, the reference signal is demodulated at the input frequency ($1f$), and the laser was locked to the zero crossing of the $1f$ demodulated reference signal. Since the reference signal is usually much stronger than the analyte signal, the lock-in amplifier can be operated with a smaller time constant (125 μs).

The molecular signal is observed for the entire lifetime of the molecular expansion, and the output of the lock-in amplifier is digitized at a rate of 25 MHz. Each trace is integrated immediately after acquisition. In a typical experiment, data from 100 gas pulses are averaged. Gas samples were either purchased from Scott Specialty Gases (CO_2 in N_2, certified), or prepared by diluting air with nitrogen. Absolute sample concentrations were derived from calibration curves.

III. RESULTS AND DISCUSSION

A. Instrument performance

1. Applicability of the molecular-beam technique to sensing

In the sample spectrum shown in Fig. 3, only the R(0) transition appears as a very intense Doppler doublet on an otherwise flat baseline. The flat baseline is a significant advantage over the normally sloped background typical of tunable diode laser spectra (see, for example, the reference spectrum in Fig. 3). The slanting arises because the diode current not only modifies the diode frequency but also the output power. The recorded reference spectrum resembles the Hitran[24] simulation in all aspects except for the sloped background. Many additional CO_2 transitions can be seen in the reference spectrum and the Hitran[24] simulation, which are not visible in the spectrum of the molecular expansion. The energy levels corresponding to these additional lines are effectively depopulated in the molecular expansion by rotational and vibrational cooling. Because we could not observe higher J transitions of CO_2, we used the line intensities of the denser spectra of van der Waals complexes to estimate the beam temperature (see below). The observed intensities are consistent with a rotational temperature of the expansion of 1–2 K.

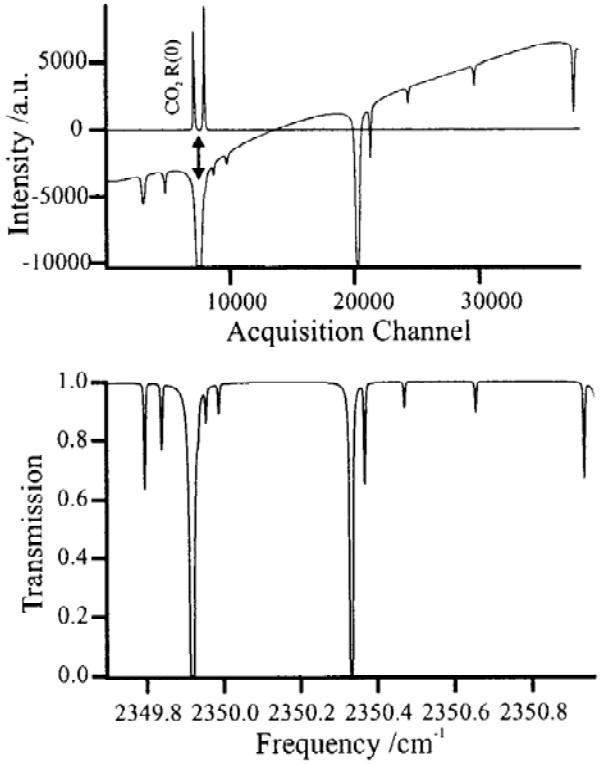

FIG. 3. Trace (a): Spectrum of a molecular expansion of CO_2 in He carrier gas. The flat baseline is a consequence of the molecular pulse on/off modulation. Only the Doppler doublet of the R(0) transition of CO_2 is visible. Trace (b): The CO_2 reference spectrum (sloped baseline) obtained from a reduced pressure static gas sample. Bottom trace: Simulated CO_2 spectrum based on the Hitran database (Ref. 24).

2. Axial versus perpendicular expansion: Line shape studies

To assess the merits of the axial nozzle arrangement, we moved the nozzle to a perpendicular position, optimized the signal intensity, and compared the results (see Fig. 4). Even though each Doppler component samples only half of the total absorption path, the intensity of the Doppler pair is approximately equal to the signal from the perpendicularly injected sample. Thus, a SN gain of a factor of about 2 is realized by moving to the axial position. This is in accord

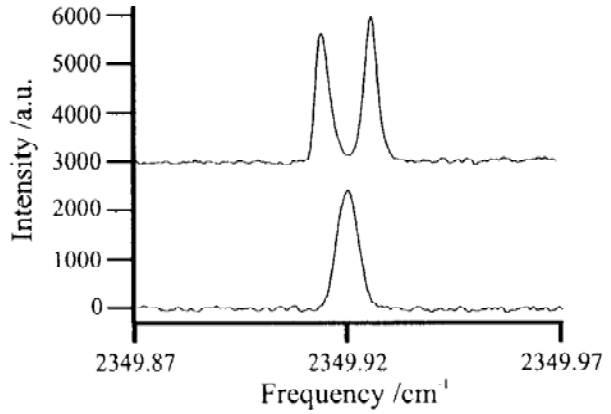

FIG. 4. The R(0) transition of CO_2 at 2349.917 cm^{-1}. The sample was air at ambient pressure. The top spectrum was obtained with the nozzle in a position axial to the optical axis, the bottom spectrum with the same nozzle in a perpendicular position. The blueshifted Doppler component is slightly more intense because of variation of the laser power with frequency.

with results obtained by Walker *et al.* in the millimeter wave region.[21] The sensitivity is improved with the axial injection because of better overlap of the laser beam with the denser portion of the molecular expansion immediately behind the nozzle and because of the longer residence time of the molecular expansion in the laser beam. However, the sensitivity cannot be arbitrarily increased by increasing the sample cell length, mainly because the density of the molecular expansion decreases along the expansion direction.

The linewidth of each Doppler component is significantly smaller than the Gaussian line shape observed in the perpendicular expansion because of a narrower velocity distribution and resulting decreased residual Doppler broadening (Fig. 4). A close inspection of the line shapes reveals that both Doppler components are somewhat broadened towards the center of the pair. A possible explanation can be found by considering the geometrical overlap of molecular expansion and laser beam. A fraction of the molecules will leave the nozzle at a relatively large angle with respect to the optical axis of the cavity. These molecules have somewhat smaller velocity components along the cavity axis than the majority, and their absorptions have, therefore, smaller Doppler shifts. This leads to a slight broadening of the Doppler components towards the center frequency. Since the peak broadening mechanism depends on the speed and shape of the molecular beam, the observed linewidths can vary with sample conditions. The line widths observed in this work are comparable to those obtained in similar work with slit nozzles.[27–29] A lower limit for the linewidth is set by the laser linewidth, which the manufacturer specified as 20 MHz.

The splitting of each transition into a Doppler doublet has several advantages. In general, the fitting of a line shape equation to two peaks simultaneously yields more precise and accurate results than those obtained from single peak fits. The doublet also allows the application of new modulation schemes (see Fig. 2 and Sec. III B 2). In addition, the Doppler doublet provides information about the beam velocity. If the beam velocity is known *a priori* or from fitting of nearby more intense transitions, the doublet line shape may lead to lower detection limits. For example, if the SNR is poor, it is generally hard to discriminate between a single peak and random spikes in the baseline. In contrast, the doublet line shape is more easily distinguished from a noisy background; for example, through automated pattern recognition algorithms. One disadvantage of the Doppler splitting is the increased spectral crowding, which complicates the analysis of closely spaced transitions; for example, in the spectra of van der Waals complexes.

3. Scan-to-scan reproducibility

One experimental parameter that affects the performance of the spectrometer is the reproducibility of the molecular pulses. We noticed that the intensity of individual transitions varied substantially from pulse to pulse, and compensated by averaging several hundred scans in each experiment. Averaging did not lead to observable line broadening, even when tens of thousands of scans were averaged over periods of several hours, indicating that the software frequency-locking procedure was working properly. Poor pulse-to-pulse reproducibility is a result of pulse-to-pulse variations of the nozzle performance. It mainly affects the amount of gas injected and also the effective beam temperature; that is, the redistribution of molecules into lower energy levels.

B. Applications

1. Weakly bound complexes

The study of weak intermolecular interactions in the gas phase has been a very active research area in the past two decades. Molecular-beam spectroscopy has become a common technique to generate, and to measure spectra of, weakly bound complexes. Lead salt diodes are often used as laser sources for mid-infrared spectroscopy of complexes,[30] despite their limited continuous tuning range of only a few wave numbers. The absorption frequency of an infrared active mode of one of the cluster constituents is only slightly perturbed by complex formation, and the B rotational constants are often small because of the typically large intermolecular separations. Thus, many infrared spectra of complexes fall within a few wave numbers of the band origin of the respective monomer vibration. Because of the occurrence of many closely spaced lines within the tuning range of the diode laser and because only a small percentage of monomer will form gas adducts in a molecular beam, van der Waals complexes are ideal to evaluate the performance of an infrared molecular-beam spectrometer in terms of sensitivity and diode laser tunability. We recorded the mid-infrared spectra of several van der Waals complexes, including Ar–CO_2,[27] $(CO_2)_2$,[28] He–CO_2,[29] and CO_2–SO_2. The first three complexes were chosen because their mid-infrared spectra are known and could serve to optimize sample conditions and to evaluate the performance of the spectrometer. For CO_2–SO_2, only its microwave spectrum was reported earlier.[31] A detailed analysis of its mid-infrared spectrum will be given elsewhere.[32]

An example spectrum of Ar–CO_2 is shown in Fig. 5. The P, Q, and R branches of the $K_a = 1 \leftarrow 0$ stack are shown.

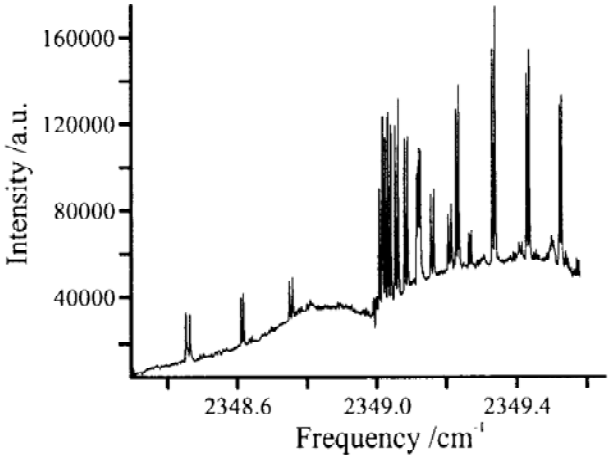

FIG. 5. A portion of the Ar–CO_2 spectrum. The sample was 8% CO_2 in Ar carrier gas at a pressure of 2 atm 2000 cycles were averaged. The $^RP_0$, $^RQ_0$, $^RR_0$ branches (from left to right) are clearly visible. The elevated background is due to the formation of higher order clusters. The negative spike at 2349.0 cm^{-1} is due to a CO_2 monomer line. Such lines are due to residual static gas present in the sampling region and were recorded during the background scan. Their observation could have been avoided by a lower molecular pulse repetition rate.

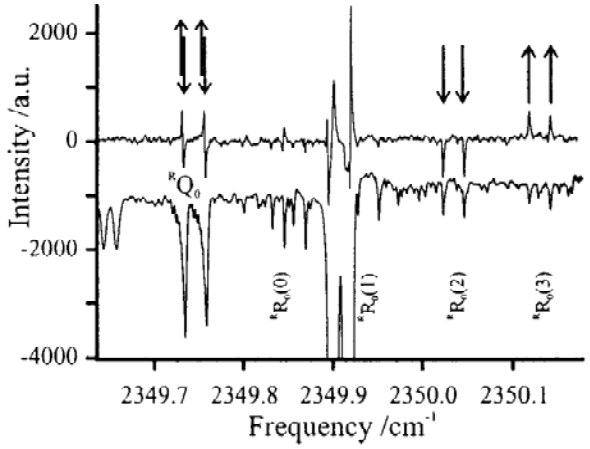

FIG. 6. Bottom trace: Portion of the CO_2–SO_2 spectrum. The strong feature at 2349.917 cm^{-1} is the $CO_2R(0)$ transition. Top trace: DR difference spectrum. The pump radiation was resonant with the $3_{03}\leftarrow2_{02}$ microwave transition at 8997.498 MHz (Ref. 31). The difference spectrum was recorded with twice the number of cycles and higher backing pressure to improve the SNR. The arrows mark the enhancement (reduction) of the intensities of the $4_{13}\leftarrow3_{03}$ ($3_{12}\leftarrow2_{02}$) and $3_{13}\leftarrow3_{03}$ ($2_{12}\leftarrow2_{02}$) infrared transitions.

This spectrum illustrates several aspects of our axial molecular beam diode laser spectrometer, among them a properly functioning frequency lock, baseline subtraction, and increased spectral congestion due to Doppler doubling. It is evident that the frequency lock is working properly because of the sharpness of the peaks even though 2000 cycles were averaged. The broad baseline features visible in the spectrum in Fig. 5 are mainly due to formation of higher order clusters, and are not a result of a failing background subtraction. The broad absorption features of atmospheric carbon dioxide and the steeply sloped background typical of diode lasers have been effectively removed by background subtraction. One must keep in mind, though, that the transition intensities shown in the spectrum are dependent on the incident laser power, which is not constant in a regular frequency scan.

In order to assess accuracy and precision of our instrument, transitions of the weakly bound dimers $(CO_2)_2$[28] and He–CO_2[29] were recorded repeatedly over a period of several days and analyzed. Frequencies of $(CO_2)_2$ could be reproduced within 0.0004 cm^{-1} of the predictions based on the previously reported spectroscopic constants.[28] Precise results were obtained because the line shape of the entire Doppler doublet was used in the numerical fit. The He–CO_2 frequencies could be reproduced to within 0.0008 cm^{-1} of the previously[29] measured values. In general, the measurement accuracy of the spectrometer is limited by the nonlinear tuning rate of the lead salt diode, which cannot be exactly expressed by the polynomial function. High uncertainty exists especially in the relative large gaps between known CO_2 transitions. We tested several different equation types, such as polynomials with variable noninteger exponents, with mixed success. Ultimately, a high finesse and low free spectral range temperature- and pressure-stabilized etalon would lead to better frequency calibration.

The linewidths of different transitions of the complexes varied substantially but reproducibly between 55 and 109 MHz FWHM for $(CO_2)_2$, and between 84 and 94 MHz FWHM for He–CO_2. CO_2 monomer lines were narrower, approximately 40 MHz FWHM. We believe that our linewidths are limited by a combination of residual laser linewidth and Doppler broadening. The latter contribution comes from the sampling of complexes with velocity components perpendicular to the slightly off-axial laser beam. The different line widths for monomer and complexes may be a result of predissociation broadening. Vibrational predissocation of the CO_2 dimer in particular has been investigated by Pine and Fraser.[33] In the original work on He–CO_2, lifetime broadening was masked by what was thought to be excess laser jitter;[29] however, lifetime broadening has been demonstrated recently by the same group for the similar complex H_2–H_2O.[34]

The CO_2–SO_2 complex has been previously studied in the microwave region.[31] During the experiments on this system, we added microwave DR capability to our spectrometer to facilitate the spectral assignment of the mid-infrared spectrum of this complex. In the MW-IR DR experiments, difference spectra were obtained by applying an on/off modulation of the microwave pump radiation for consecutive molecular pulses. The effect of the microwave radiation is a shift in the relative populations of the two energy levels involved. For example, if a J=3–2 rotational transition is pumped, the intensity of an infrared transition originating from the J=2 level in the ground vibrational state is reduced, while the intensity of an infrared transition originating from the J=3 level is increased (see Fig. 6). We found that occasionally the populations of neighboring J levels were also affected, probably attributable to collisional population transfer during the early stages of the molecular expansion. In general, the difference spectra were relatively noisy because of incomplete cancellation of peaks in the background subtraction. Strong peaks like the CO_2 R(0) line in particular did not subtract entirely, mainly because of pulse-to-pulse variations in the molecular expansion.

A significant number of lines are visible in the bottom spectrum in Fig. 6, a result of simultaneous observation of CO_2 monomer and CO_2–SO_2 dimer transitions. At a microwave frequency resonant to the $3_{03}\leftarrow 2_{02}$ pure rotational transition, the difference spectrum (top trace in Fig. 6) shows only the intensity enhancements (reductions) at the $4_{13}\leftarrow 3_{03}$ ($3_{12}\leftarrow 2_{02}$) and $3_{13}\leftarrow 3_{03}$ ($2_{12}\leftarrow 2_{02}$) infrared transitions (marked by arrows). Due to the high selectivity of the microwave-infrared double resonance experiment, very closely spaced lines can be distinguished from each other. This is apparent in the $^{R}Q_0$ branch (Fig. 6) of CO_2–SO_2. The closely spaced $2_{12}\leftarrow 2_{02}$ and $3_{13}\leftarrow 3_{03}$ transitions are easily distinguishable in the difference spectrum, but cannot be distinguished in the single-resonance infrared experiment. We found that the microwave frequency could be detuned by up to 0.5 MHz before a noticeable reduction of the difference signal was observed. Microwave pump power of less than 0.5 mW was sufficient to detect DR effects.

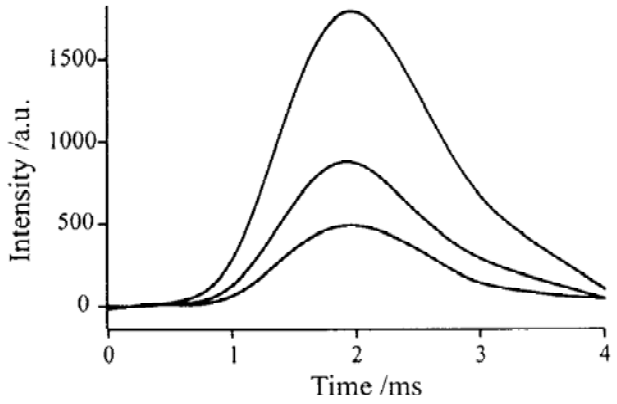

FIG. 7. Representative response curves of the spectrometer operated in frequency–2 f-demodulation mode, averaged over 100 molecular pulses. The samples were (top to bottom) 150, 61, and 25 ppb CO_2 in nitrogen at pressures of 1 atm. The pulse nozzle was triggered at time zero. The response curve corresponds to the appearance of the molecular expansion in the sampling area.

2. Trace gas sensing

The cooling of rotational degrees of freedom in the molecular beam is expected to eliminate spectral interference from major atmospheric components such as water and carbon dioxide. Water vapor is especially problematic in trace-gas-sensing applications because its RT absorption spectrum covers large regions of the mid-infrared. Since the water vapor concentration in air can fluctuate considerably, large regions of the mid-infrared are rendered essentially useless from an analytical viewpoint. The narrower line widths and the depopulation of higher J levels in the molecular expansion allows in principle a much wider range of the mid-infrared to be accessible for trace-gas-sensing compared to atmospheric pressure, or even reduced pressure, applications.

Carbon dioxide is the second most abundant infrared-absorbing molecule in the atmosphere. It is also a strong absorber, and is therefore relatively easy to detect. Its non-toxic nature and availability, in particular in the form of certified standards, make it an ideal test molecule for any gas sensor. There is also some renewed interest in accurate and precise measurement methods of greenhouse gases like CO_2, in light of the Rio Declaration[35] and the Kyoto protocol.[36] In the last five years, a number of near-infrared diode laser spectrometers have been constructed specifically for the purpose of CO_2 sensing.[37–41] Mid-infrared spectrometers, such as the one recently described by Roller *et al.*,[17] are in principle more sensitive than their near-infrared counterparts because of the typically larger absorption coefficients in the mid-infrared. In the following we demonstrate the suitability of a mid-infrared pulsed molecular-beam spectrometer for precision measurements of gas concentrations.

For the trace-gas-sensing application, the spectrometer was operated in single-frequency mode as described in Sec. II B. In this mode, the 2 f-demodulated signal is sampled, typically at a rate of 25 MHz, for the entire lifetime of the molecular expansion. Figure 7 shows signals obtained after averaging over 100 molecular pulses. The sample concentrations were 150, 61, and 25 ppb (top to bottom traces), respectively. Time zero marks the point when the pulse nozzle is triggered. The molecular signal appears about 0.5 ms after the trigger. The signal becomes slightly negative at the end of the pulse lifetime of about 4 ms as a result of static gas in the sample cell that is no longer traveling in the direction of the gas expansion and is therefore not Doppler split. The experiments shown in Fig. 7 were reproducible within 6% relative standard deviation. The overall instrumental limit of detection is estimated to be in the sub-ppb range.

The run-to-run reproducibility of the pulsed molecular-beam spectrometer was limited by gas delivery variations and laser diode instability. Frequency fluctuations of the laser diode could be reduced by locking the diode to the R(0) monomer transition. Small residual laser frequency fluctuations were unavoidable due to the finite response time of the stabilizing feedback circuit. Much larger run-to-run variations resulted from irreproducible sample gas delivery through the pulse nozzle, which fluctuated by up to 30% between runs. These fluctuations were essentially random and were effectively eliminated by averaging over several hundred molecular pulses.

ACKNOWLEDGMENTS

This project was supported by the Canadian Institute for Photonic Innovations, one of the national Networks of Centres of Excellence in Canada, the Alberta Science and Research Authority, and the Natural Sciences and Engineering Research Council of Canada (NSERC). One of the authors (H. D. O.) gratefully acknowledges graduate scholarships from the Alberta Ingenuity Fund and NSERC. The authors thank R. Lipiecki for constructing several elements of the spectrometer and M. C. L. Gerry, University of British Columbia, for the loan of a microwave synthesizer.

[1] A. De Piante, E. J. Campbell, and S. J. Buelow, Rev. Sci. Instrum. **60**, 858 (1989).
[2] Z. Wang, M. Eliades, K. Carron, and J. W. Bevan, Rev. Sci. Instrum. **62**, 21 (1991).
[3] T. A. Hu, E. L. Chappel, and S. W. Sharpe, J. Chem. Phys. **98**, 6162 (1993).
[4] I. Pak, M. Hepp, D. A. Roth, and G. Winnewisser, Rev. Sci. Instrum. **68**, 1668 (1997).

[5] J. Faist, F. Capasso, D. L. Sivco, C. Sirtori, A. L. Hutchinson, and A. Y. Cho, Science **264**, 553 (1994).
[6] D. Herriott, H. Kogelnik, and R. Kompfner, Appl. Opt. **3**, 523 (1963).
[7] J. Altmann, R. Baumgart, and C. Weitkamp, Appl. Opt. **20**, 995 (1981).
[8] J. U. White, J. Opt. Soc. Am. **66**, 411 (1976).
[9] D. Kaur, A. M. de Souza, J. Wanna, S. A. Hammad, L. Mercorelli, and D. S. Perry, Appl. Opt. **29**, 119 (1990).
[10] J. B. McManus, P. L. Kebabian, and M. S. Zahniser, Appl. Opt. **34**, 3336 (1995).
[11] C. M. Lovejoy and D. J. Nesbitt, Rev. Sci. Instrum. **58**, 807 (1987).
[12] P. Werle, Spectrochim. Acta, Part A **52**, 805 (1996); Spectrochim. Acta, Part A **54**, 197 (1998).
[13] P. Werle, K. Maurer, R. Kormann, R. Mücke, F. D'Amato, and A. Popov, Spectrochim. Acta, Part A **58**, 2361 (2002).
[14] M. Loewenstein, H. Jost, J. Grose, J. Eilers, D. Lynch, S. Jensen, and J. Marmie, Spectrochim. Acta, Part A **58**, 2329 (2002).
[15] G. Toci, P. Mazzinghi, B. Mielke, and L. Stefanutti, Opt. Lasers Eng. **37**, 459 (2002).
[16] D. Richter, M. Erdelyi, R. F. Curl, F. K. Tittel, C. Oppenheimer, H. J. Duffell, and M. Burton, Opt. Lasers Eng. **37**, 171 (2002).
[17] C. Roller, K. Namjou, J. Jeffers, W. Potter, P. J. McCann, and J. Grego, Opt. Lett. **27**, 107 (2002).
[18] T. J. Balle and W. H. Flygare, Rev. Sci. Instrum. **53**, 33 (1981).
[19] J.-U. Grabow and W. Stahl, Z. Naturforsch., A: Phys. Sci. **45**, 1043 (1990).
[20] Y. Xu and W. Jäger, J. Chem. Phys. **106**, 7968 (1997).
[21] K. A. Walker and A. R. W. McKellar, Molecul. Spectrosc. **205**, 331 (2001).
[22] H. D. Osthoff, W. Jäger, J. Walls, and W. A. van Wijngaarden, Proc. SPIE **4817**, 249 (2002).
[23] J. B. McManus and P. L. Kebabian, Appl. Opt. **29**, 898 (1990).
[24] http://www.hitran.com. The software package Hitran-PC 2.51 (http://www.ontar.com) was used for simulations.
[25] W. H. Press, S. A. Teukolsky, W. T. Vetterling, and B. P. Flannery, *Numerical Recipes in C*, 2nd ed. (Cambridge University Press, Cambridge, UK, 1999), p. 547.
[26] R. G. Brown, *Introduction to Random Signal Analysis and Kalman Filtering* (Wiley, New York, 1983).
[27] R. W. Randall, M. A. Walsh, and B. J. Howard, Faraday Discuss. Chem. Soc. **85**, 13 (1988).
[28] M. A. Walsh, T. H. England, T. R. Dyke, and B. J. Howard, Chem. Phys. Lett. **142**, 265 (1987).
[29] M. J. Weida, J. M. Sperhac, D. J. Nesbitt, and J. M. Hutson, J. Chem. Phys. **101**, 8351 (1994).
[30] G. Winnewisser, T. Drascher, T. Giesen, I. Pak, F. Schmulling, and R. Schieder, Spectrochim. Acta, Part A **55**, 2121 (1999).
[31] L. Sun, I. I. Ioannou, and R. L. Kuczkowski, Mol. Phys. **88**, 255 (1996).
[32] H. D. Osthoff and W. Jäger (unpublished).
[33] A. S. Pine and G. T. Fraser, J. Chem. Phys. **89**, 100 (1988).
[34] M. J. Weida and D. Nesbitt, J. Chem. Phys. **110**, 156 (1999).
[35] *Agenda 21 and The UNCED Proceedings*, edited by N. A. Robinson (Oceana, New York, 1992).
[36] M. Grubb, *The Kyoto Protocol: A Guide and Assessment* (The Royal Institute of International Affairs, London, 1999).
[37] R. M. Mihalcea, M. E. Webber, D. S. Baer, R. K. Hanson, G. S. Feller, and W. B. Chapman, Appl. Phys. B: Lasers Opt. **67**, 283 (1998).
[38] P. Werle, R. Mücke, F. D'Amato, and T. Lancia, Appl. Phys. B: Lasers Opt. **67**, 307 (1998).
[39] L. Gianfrani, P. De Natale, and G. De Natale, Appl. Phys. B: Lasers Opt. **70**, 467 (2000).
[40] G. Gagliardi, R. Restieri, G. De Biasio, P. De Natale, F. Cotrufo, and L. Gianfrani, Rev. Sci. Instrum. **72**, 4228 (2001).
[41] M. E. Webber, R. Claps, F. V. Englich, F. K. Tittel, J. B. Jeffries, and R. K. Hanson, Appl. Opt. **40**, 4395 (2001).